ISSN 1996-5052

Current Research in Chemistry

http://knowledgiascientific.com

Knowledgia SCIENTIFIC
A Place to Publish Outstanding Research

Current Research in Chemistry 3 (1): 29-48, 2011
ISSN 1996-5052 / DOI: 10.3923/crc.2011.29.48

Microstructure and Current-voltage Characteristics of (ZnO-CuO) Varistor System in the Presence of Additive Oxides, Cr_2O_3, Bi_2O_3 and NiO

[1]S.E. Mansour, [1]O.A. Desouky, [2]S.M. Negim and [2]W.A. Kamil
[1]Department of Chemistry, Faculty of Science, Omar Al-Mukhtar University, Box 919, Al-Bayda, Libya
[2]School of Chemical Sciences, Universiti Sains Malaysia, 11800, Penang, Malaysia

Corresponding Author: Dr. Saber E. Mansour, Department of Chemistry, Faculty of Science, Omar Al -Mukhtar University, Box 919, Al-Bayda, Libya Tel: +218-91-3767134

ABSTRACT

The microstructure, electrical properties and density of ZnO-based varistor ceramics with different CuO content prepared by ball milling and sintered at (900-1200°C) were investigated. The nonlinear coefficient (α) and density increase with increasing CuO content. The presence of a liquid phase facilitated the sintering process and developed atomically interfaces, uniform intergranular phase required for non-linear conduction. The presence of Cr_2O_3 in group (II) absent of grain growth (inhibition of grain growth) and enter in solid solution with ZnO. X-ray diffraction analysis of sintered samples reveals no formation of new phases, but lattice constants of the phases were changed after sintering.

Key words: Varistor, electrical properties, ZnO, ceramics

INTRODUCTION

Varistors are materials with nonlinear current-voltage characteristics. They are used both as protecting devices against over voltages in electronic and industrial equipments and as surge arrestors (Souza *et al.*, 2003). Commercial varistors used in protection systems are based on SiC (silicon carbide) or ZnO (zinc oxide). SiC-based varistors have low nonlinearity coefficients ($\alpha = 5$) where α is the nonlinearity constant defined by the relation: $I = K V \alpha$, where I is current, V is voltage and K is a proportionality constant (Skuratovsky *et al.*, 2004). The ZnO-based varistors have very high nonlinearity coefficients ($\alpha = 50$) and their major phase contains (besides ZnO) small amounts of Bi_2O_3, Sb_2O_3, CoO, MnO_2 and Cr_2O_3 (Tong *et al.*, 2009; Wu *et al.*, 2010). The reaction between the ZnO and the additives at high temperatures leads to the formation of several phases at the ZnO grain boundaries (Peiteado *et al.*, 2005). Thus, despite their chemical composition and phases, the processing method as well as the sintering temperature, heating and cooling rates influence the electrical properties of these ceramics fundamentally (Lin *et al.*, 2007). In view of this fact, the literature contains extensive reports describing the influence of processing variables on the properties and mechanisms that govern these system properties (Bernik and Daneu, 2007; Ott *et al.*, 2001; Cong *et al.*, 2007; So and Park, 2002; Nahm, 2004, 2007). Other varistor systems based on $SrTiO_3$ (Skuratovsky *et al.*, 2006) or TiO_2 (Glot and Skuratovsky, 2006; Antunes *et al.*, 2002; Leach, 2005) have been described in the literature, but the nonlinearity of

these systems is around ($2<\alpha<12$), which is lower compared to that of the multicomponent ZnO varistors. Rare earth elements can improve E_b of ZnO based varistor ceramics (Bernik *et al.*, 2004) and other properties of various varistors (Santos *et al.*, 2001; Wang *et al.*, 2005). The ZnO varistor ceramics with Y_20_3 added exhibited improved E_b(Glot, 2006a; Wang *et al.*, 2000) reported that addition of rare earth oxides RE,O, (RE = Er, Y, Dy) to Zn0-Pr_6O_{11}-based varistors improved both E_b and nonlinearity. However, they all used traditional ball milling or low-energy ball milling and high-temperature sintering methods, which bore no advantage in both technology and economy.

MATERIALS AND METHODS

Experimental procedures: Reagent grade ZnO and one or more additive oxides of type CuO, Bi_2O_3, Cr_2O_3 and NiO were mixed in the desired proportion and ball Milled for 2 h. Five series of mixes were suggested to study the effect of copper oxide alone in a binary system ZnO plus CuO and in the presence of additive oxides, Cr_2O_3, Bi_2O_3 and NiO according to Table 1. The mixture was then pressed into discs and sintered at temperatures of 900 to 1200°C in air. The final dimensions of the samples were 1.2 cm diameter and 0.2 cm thickness. The sintered samples were lapped to remove surface flaws and an ohmic contact was provided on both surfaces by coating with silver paint. The samples thus prepared could be used for measurement of electrical properties such as V-I characteristics. The V-I measurements of the samples were made by using a dc power supply in current range up to 2 mA and pulse technique for higher current ranges. The electric circuit of the varistor sample is shown in Fig. 1.

The non-linearity index (α) was calculated in a current range of 1 mA to 1 A using the following equation:

$$\alpha = (\log I_2 - \log I_1) / (\log V_2 - \log V_1)$$

where, I_1 and I_2 are the currents at the voltages V_1 and V_2.

The phase composition of the samples was analyzed by X-ray diffraction (XRD) using Cu Kα radiation on a power diffractometer (Philips apparatus type 170). Samples for microstructure analysis were polished on the plane surface with carborundum paper of different grades 300, 600 and 1000 followed grades of diamond paste 7, 2.5 and 1 micron. The samples were then thoroughly washed in an ultrasonic bath for half an hour. The polished samples were etched in 5% dilute HCl solution for 5 sec. Microstructure developed was examined under SEM type Philips XL 30 provided with EDAX, after sputtering with gold.

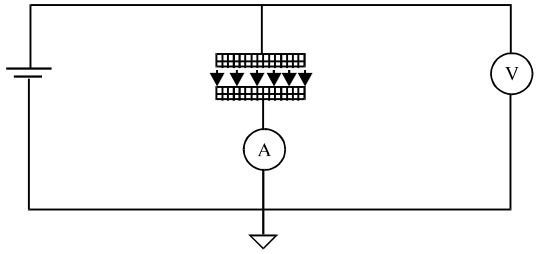

Fig. 1: The position of varistor sample in electric circuit

Table 1: Composition of different mixes in mol %

Oxides	ZnO mol%	CuO mol%	Cr_2O_3 mol%	Bi_2O_3 mol%	NiO mol%
Group (I)					
M0	100.0	0.0	-	-	-
M1	99.7	0.3	-	-	-
M2	99.5	0.5	-	-	-
M3	99.0	1.0	-	-	-
M4	98.0	2.0	-	-	-
M5	97.0	3.0	-	-	-
M6	96.0	4.0	-	-	-
M7	95.0	5.0	-	-	-
M8	94.0	6.0	-	-	-
Group (II)					
A1	99.2	0.3	0.5	-	-
A 2	99.0	0.5	0.5	-	-
A 3	98.5	1.0	0.5	-	-
A 4	97.5	2.0	0.5	-	-
A 5	96.5	3.0	0.5	-	-
A 6	95.5	4.0	0.5	-	-
A 7	94.5	5.0	0.5	-	-
A 8	93.5	6.0	0.5	-	-
Group (III)					
Z1	99.2	0.3	-	0.5	-
Z 2	99.0	0.5	-	0.5	-
Z 3	98.5	1.0	-	0.5	-
Z 4	97.5	2.0	-	0.5	-
Z 5	96.5	3.0	-	0.5	-
Z 6	95.5	4.0	-	0.5	-
Z 7	94.5	5.0	-	0.5	-
Z 8	93.5	6.0	-	0.5	-
Group (VI)					
C1	99.2	0.3	-	-	0.5
C2	99.0	0.5	-	-	0.5
C3	98.5	1.0	-	-	0.5
C4	97.5	2.0	-	-	0.5
C5	96.5	3.0	-	-	0.5
C6	95.5	4.0	-	-	0.5
C7	94.5	5.0	-	-	0.5
C8	93.5	6.0	-	-	0.5
Group (V)					
B	92.5	6.0	0.5	0.5	0.5

RESULTS

Sinterability of the suggested mixes is deuced from the results of physical properties in terms of water absorption, apparent porosity, bulk density and firing shrinkage. Results of firing shrinkage and bulk density showed an increase with rise in temperature. Maximum values of firing shrinkage were attained in specimens fired at 1200°C for 2 h. Firing the specimens more than 1100°C for 2 h caused the start of deformation of the different mixes. Therefore, it is not recommended to increase the temperature more than 1100°C as the increase in bulk density

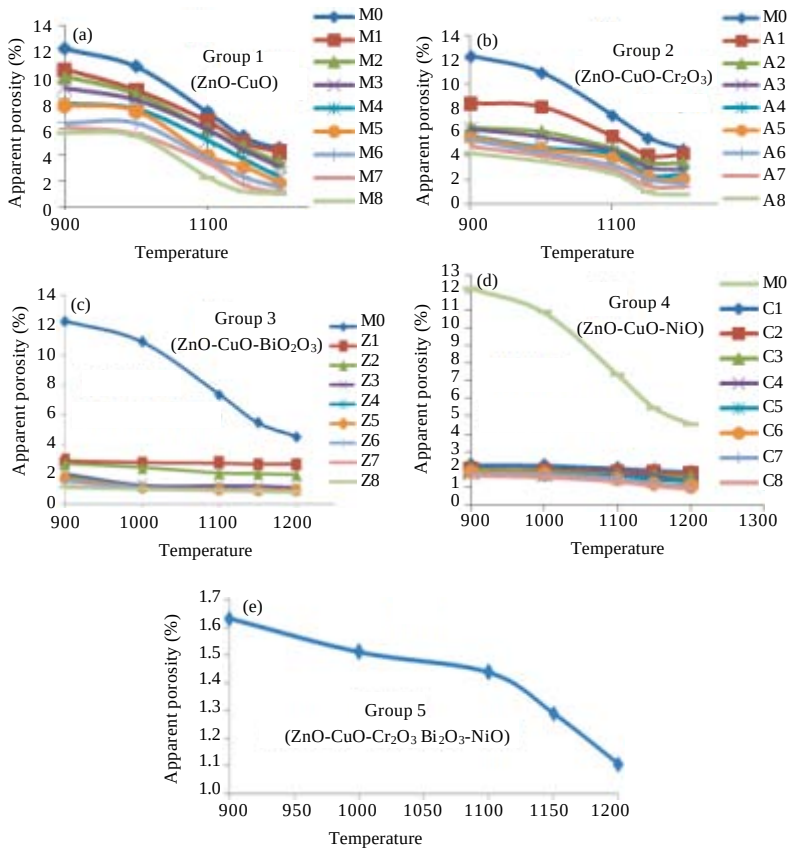

Fig. 2: (a-e) Apparent porosity of different groups

displayed there did not show remarkable change with increasing temperature. Addition of 0.5 mol % Bi_2O_3 with increase the content of CuO lead better densification. CuO improves densification by minimizing the present of closed pores. Water absorption of group (V) is less than of group (III) and group IV, i.e., addition of 0.5 mol % of each oxide (Cr_2O_3+ Bi_2O_3+NiO) with increase the content of CuO lead better densification as shown in Fig. 2.

X-ray diffraction analysis of sintered samples reveals no formation of new phases, but lattice constants of the phases were changed after sintering. Lattice constants of each sample were changed in different extents depending on the phase's affinity to a particular ion and on overall varistor composition. XRD patterns of the respective mixes fired at 1100°C for 2 h, showed a shift in the d-spacing equivalent to (0.02-0.04)°A in the main ZnO peak indicating a kind of limited solid solution of CuO in the oxide . A maximum shift of 0.04°A was recorded in mix containing 6 mol % CuO, XRD results of group (II) which containing 0.5 mol % Cr_2O_3, showed that no binary compound was formed. The electronic defects are introduced by adding minor dopants such as the oxides of Bi, Co, Mn and Cr. The effects of dopants are classified into three categories. The first are additives forming the basic microstructure (Glot, 2006b; Ramirez *et al.*, 2005; Simoes *et al.*, 2003; Yongjun *et al.*, 2000) of the sintered body, such as Bi_2O_3 and BaO. The second are additives used for the improvement of nonohmic properties, such as CoO and MgO. The third are additives used for the improvement of reliability (Oliveira *et al.*, 2003; Takemura et *al.*, 1986) such as NiO and

glass frit. The role of metal oxide can be predicted to be a source of oxygen which will be chemisorbed at ZnO grain boundaries. This chemisorbed oxygen will generate the electronic interface states at the grain boundaries (Parra *et al.*, 2005).

The role of monovalent ions is of particular interest. Although, such ions should formally behave as acceptor in ZnO, all attempts to produce P-type behaviour by doping in single crystal and films (Fayat and Castro, 2003) have failed. Thus, it is unlikely that they can act as acceptors in varistors. Some insight as to how they may substitute into ZnO comes from recent atomistic simulations (Li *et al.*, 2002). These indicated that the lowest solution energy is associated with their being amphoteric dopants, creating both substitutional and interstitial ions.

Thus, for Na_2O in corporation:

$$Na_2O \leftrightarrow Na_{Zn} + Na_i^* + ZnO^-$$

De la Rubia *et al.* (2004), reported that, monovalent ions (Li^+) tend to increase the resistivity of doped sintered poly crystalline ZnO by creating electron traps and trivalent ions (i.e., Al^{3+} and Cr^{3+}) to decrease it by supplying extra conduction electron.

The deep or shallow trap levels commonly found in bulk ZnO are as interstitial Zinc, oxygen vacancy and impurity induced donor or acceptor levels (Wang *et al.*, 2003, 2005). It is known that the manganese oxide in ZnO varistors drastically improve the nonlinear (V-I) characteristics (Batzill and Diebold, 2005).

The equilibrium between di- and trivalent manganese oxide in oxygen atmosphere is expressed by the equation (Bueno *et al.*, 2005).

$$4\,Mn_3O_4 + O_2 \xrightarrow{537^\circ C} 6\,Mn_2O_3 \xrightarrow{959^\circ C} 4\,Mn_3O_4 + O_2$$

Mn_3O_4 doping on ZnO is expected to cause interesting phenomena in relation to the point defect formation in poly crystalline ZnO.

Metz *et al.* (2007) reported that, the varistors without Al content exhibited poor non-linear characteristics as only 19.8 in non linear coefficient. However, the non-linear characteristics were greatly enhanced in nonlinear coefficient above 30 by incorporation of $Al(NO_3)_3.\ 9H_2O$. The Al atoms would act as donors. Al_2O_3 doping of ZnO is likely to involve accommodation of Al ions on host lattice sites. In this case, a trivalent Al^{3+} ion will replace a divalent Zn^{2+} ion allowing an electron to move the conduction band and the reaction can be written as follows:

$$\tfrac{1}{2}\,Al_2O_3 \leftrightarrow Al_{Zn^\circ} + e + ZnO + \tfrac{1}{4}\,O_2$$

The similar behaviour was observed in the present study with CuO and Cr_2O_3 and NiO i.e.,

$$\tfrac{1}{2}\,Cr_2O_3 \leftrightarrow Cr_{Zn^\circ} + e + ZnO + \tfrac{1}{4}\,O_2$$

This gives a net increase in the concentration of electrons, Thereby increasing the electrical conductivity of the grains, i.e., decreasing the resistance of ZnO grains, which cause an increase in non linear coefficient and leakage current.

The (V-I) Characteristics were measured at voltage between (0-5) KV and current between (0-10) mA. The effect of CuO alone is demonstrated in mixes of group (I). (V-I) characteristics of

Table 2: The non linearity of group I

CuO content (%)	α 900°C	α 1000°C	α 1100°C	α 1150°C	α 1200°C
0.0	11.21	12.49	13.58	11.36	10.06
0.3	21.70	25.90	41.90	39.80	30.70
0.5	28.10	41.50	45.60	40.70	37.80
1.0	45.70	47.20	49.50	45.30	43.90
2.0	54.00	55.50	50.30	55.20	47.80
3.0	64.98	58.60	54.80	60.50	51.60
4.0	66.10	64.99	59.60	68.60	43.20
5.0	34.70	54.40	48.00	27.50	23.30
6.0	23.30	48.50	47.30	22.40	20.70

Table 3: The non linearity of group II

CuO content (%)	α 900°C	α 1000°C	α 1100°C	α 1150°C	α 1200°C
0.0	11.21	12.49	13.58	11.36	10.06
0.3	40.30	43.30	42.10	33.90	30.20
0.5	51.60	54.20	55.50	51.20	51.53
1.0	60.20	64.50	64.50	61.24	67.28
2.0	69.01	75.60	65.60	64.61	70.86
3.0	71.01	80.20	75.80	72.08	73.88
4.0	78.42	83.70	80.90	80.22	43.50
5.0	73.02	74.70	79.80	34.12	21.40
6.0	63.15	72.40	42.20	29.04	20.98

Table 4: The non linearity of group III

CuO content (%)	α 900°C	α 1000°C	α 1100°C	α 1150°C	α 1200°C
0.0	11.21	12.49	13.58	11.36	10.06
0.3	29.20	39.03	44.10	48.40	46.50
0.5	30.42	44.01	48.10	52.50	51.50
1.0	46.60	54.44	53.99	56.50	54.30
2.0	54.01	56.72	56.10	61.40	65.02
3.0	62.79	63.62	58.80	64.10	68.80
4.0	62.85	63.10	63.60	68.60	73.68
5.0	36.80	37.04	50.90	58.80	66.16
6.0	33.60	33.71	48.97	52.20	54.41

group (I) all mixes exhibit non-ohmic relation demonstrated by the values calculated for (α) in Table 1. Mixes of group (II) representing ZnO + CuO and 0.5 % mol Cr_2O_3 additives show very good plateau in (V-I) relation with increase in the percentage of CuO beginning at 10 μA m^{-2}, which present in Fig. 3. Similar curves were obtained for group (III, IV and V) representing ZnO + CuO and 0.5% mol Bi_2O_3, ZnO+CuO and 0.5% mol NiO and ZnO + CuO and 0.5% mol Cr_2O_3+0.5% mol Bi_2O_3 + 0.5% mol NiO, respectively. The characteristic curves of different groups are greatly divided into two regions, that is, prebreakdown at low voltage region and an off-state and nonlinear properties as an on-state high voltage region, the sharper the knee of the curves between the two regions, the better the non-linearity. Table 2-6, show the variation of nonlinear exponent as function of CuO content of different mixes for all groups at different temperatures. Table 2 illustrated that, the calculated (α) in ZnO ceramic with CuO only in group (I) was from 10-65, achieving maximum 65 in CuO content of 4% mol, which fired at 1100°C for 2 h. The same

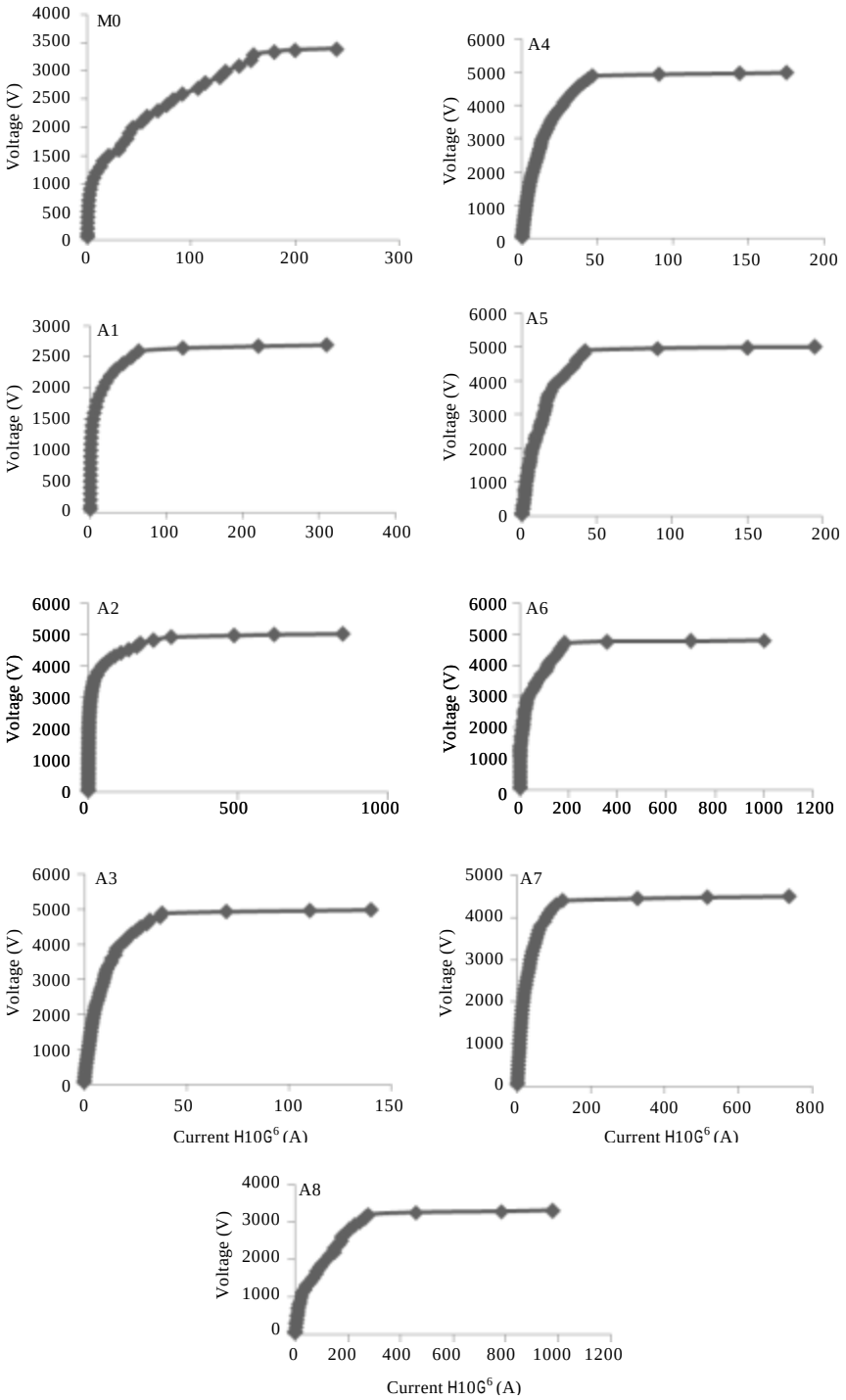

Fig. 3: (I-V) Characteristics of group II (ZnO-CuO-Cr_2O_3) at 1100°C

Table 5: The non linearity of group IV

CuO content (%)	α 900°C	α 1000°C	α 1100°C	α 1150°C	α 1200°C
0.0	11.21	12.49	13.58	11.36	10.06
0.3	49.30	54.98	69.80	62.30	55.30
0.5	64.70	70.20	73.20	71.40	61.80
1.0	70.10	72.30	80.40	80.90	74.70
2.0	78.50	81.80	88.90	84.50	81.30
3.0	90.80	95.20	100.20	100.10	99.80
4.0	93.30	103.10	115.60	109.60	103.50
5.0	88.30	104.40	104.10	81.50	73.60
6.0	82.80	95.70	69.30	65.80	67.00

Table 6: The non linearity of group V

α 900°C	α 1000°C	α 1100°C	α 1150°C	α 1200°C
73.9	92.6	114.2	120.8	87.01

behaviour was observed in Table 3-6, the calculated (α) in ZnO ceramic with different additives from 10-80, 10-75, 10-110 and 60-120 for group II, III, IV and V respectively. The value of (α) was increased with increasing CuO content until 4 mol% for all different groups, which fired at 1100°C 2 h. It can be forecasted that the ZnO-ceramics doped with 4% mol CuO and other additives should exhibit the best nonlinear properties because it has the sharpest knee. Adding of more CuO, the knee gradually becomes less pronounced and the non-linear properties reduce.

Microstructure of ZnO ceramics play an important role in the electric characteristic displayed. There are two models postulated to describe the microstructure of ZnO depending on the constitution. The present study reveals that the addition of CuO leads to a two phase microstructure; well crystalline ZnO grains in preferred orientation, ZnO crystallize in hexagonal system. It is characterized by perfect cleavage plane along 001 which was distinct in SEM of ZnO. SEM of disc specimens fired at the selected maturing temperature and thermally etched at 1000°C for 15 min are demonstrated in Fig. 4-13. The SEM of mix M0 shows ZnO grain of various sizes (2 and 5 μm). Submicron pores occur at triple points at the grain corners, which ZnO-ZnO grain junctions are devoid of them.

The SEM of mix M_1 of group (I) Fig. 6, showed a homogeneous primary particle size of 2-5 μm, ZnO grains dissolution of CuO between ZnO grains. Zinc oxide agglomerates of various sizes and shapes, some of these agglomerates are dissected and fine grains are incorporated within these lines of dissection.

The SEM of mix M_6 which containing ZnO and 4% mol CuO shows a mass of solid solution of ZnO and CuO in some places are rich in (Zn) other in (Cu) show in a kind of stereotions (dark and light lines), the mass is dissected by parallel caveats perpendicular to the lines of stereotions. The increases percentage of CuO increases the dissolution of CuO between ZnO-ZnO grains.

The presence of Cr_2O_3 leading to absent of grain growth (inhibition of grain growth) and enter in solid solution with ZnO, dark pores which present in SEM of samples A_1 and A_6 due to volatility of ZnO, as can be in Fig. 7 and 8.

SEM of mix Z_1 which containing ZnO, 0.3% mol CuO and 0.5% mol Bi_2O_3 present in Fig. 9, shows liquid phase in the triple points appears as white spots. ZnO grains are tending together and growing in size 10 nm and presence of pores of various sizes indicating a kind of volatilization. Some grains are found together forming masses that are dissected by cracks (flows).

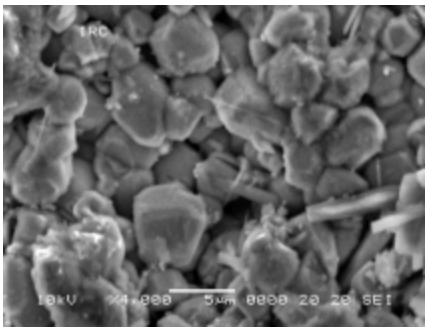

Fig. 4: SEM of ZnO, thermally etched surface, X = 4000

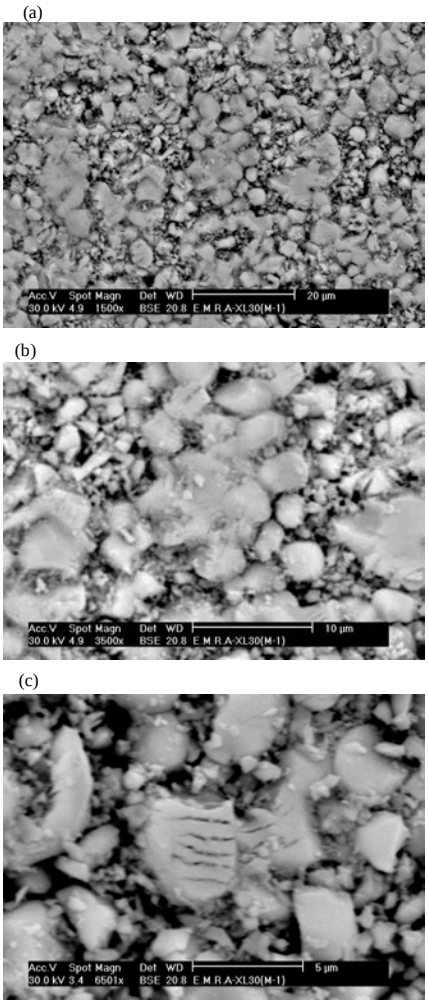

Fig. 5: SEM of M_1, group 1. Thermally etched surface, general view X = 1500. Thermally etched, fired at 1100°C showed ZnO two phases grains agglomerates of various size and intergranular phase at triple point. X= 3500. Thermally etched, showed two phases ZnO grain and intergranular phase. X = 6500

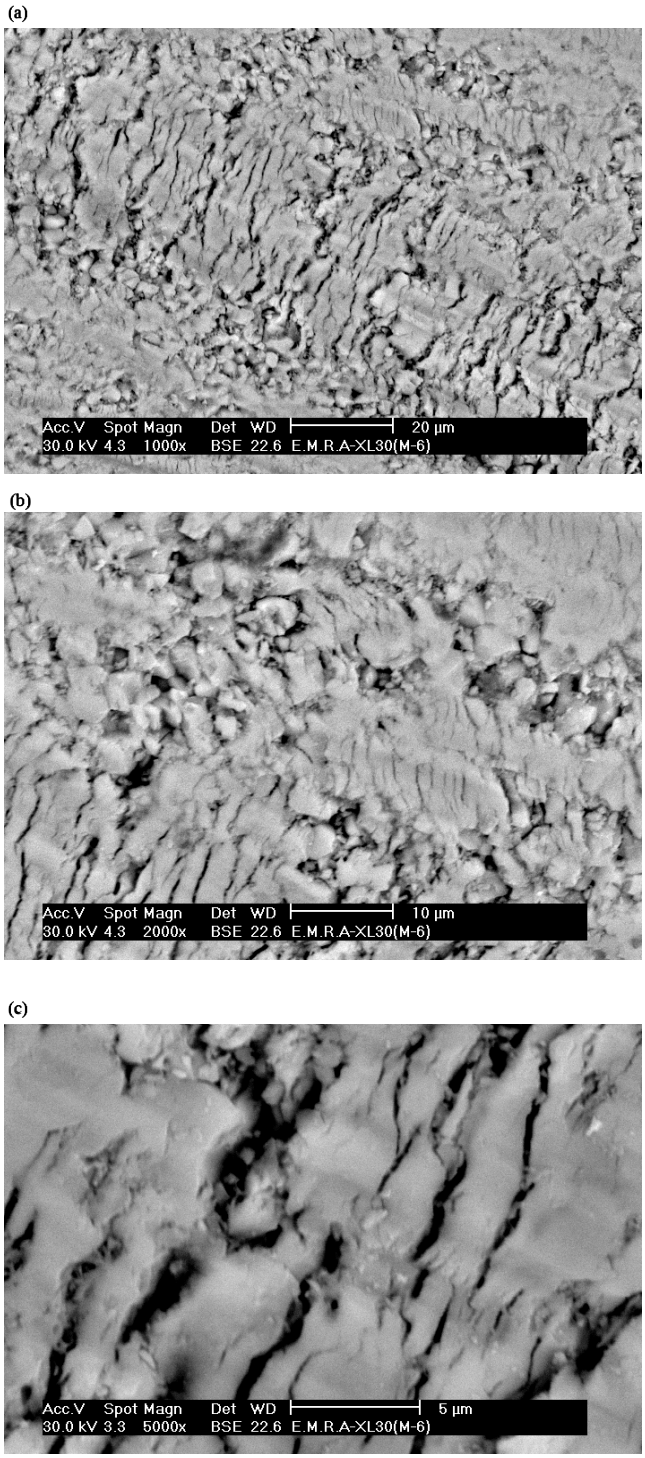

Fig. 6: SEM of mix M_6, group 1. (a) Thermally etched, general view X = 1000, (b) Thermally etched, shows a mass of solid solution of ZnO and CuO. X = 2000 and (c) Thermally etched, showed segregations along grain boundaries. X = 5000

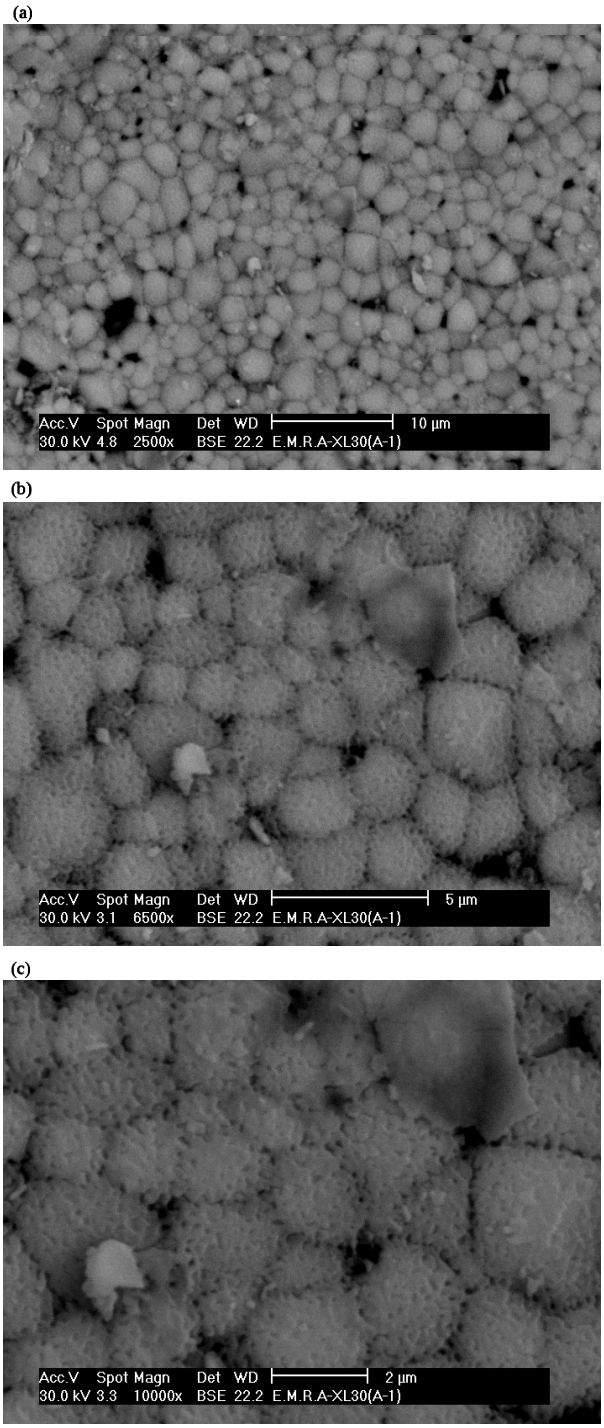

Fig. 7: SEM of mix A1, group 2. (a) Thermally etched surface, general view X = 2500 (preferred orientation in ZnO grain), (b) Thermally etched surface, showing aggregated, often submicrometer, primary particles. X = 6500 and (c) Thermally etched, showing actually agglomerates of ZnO grains (very pure fine materials)

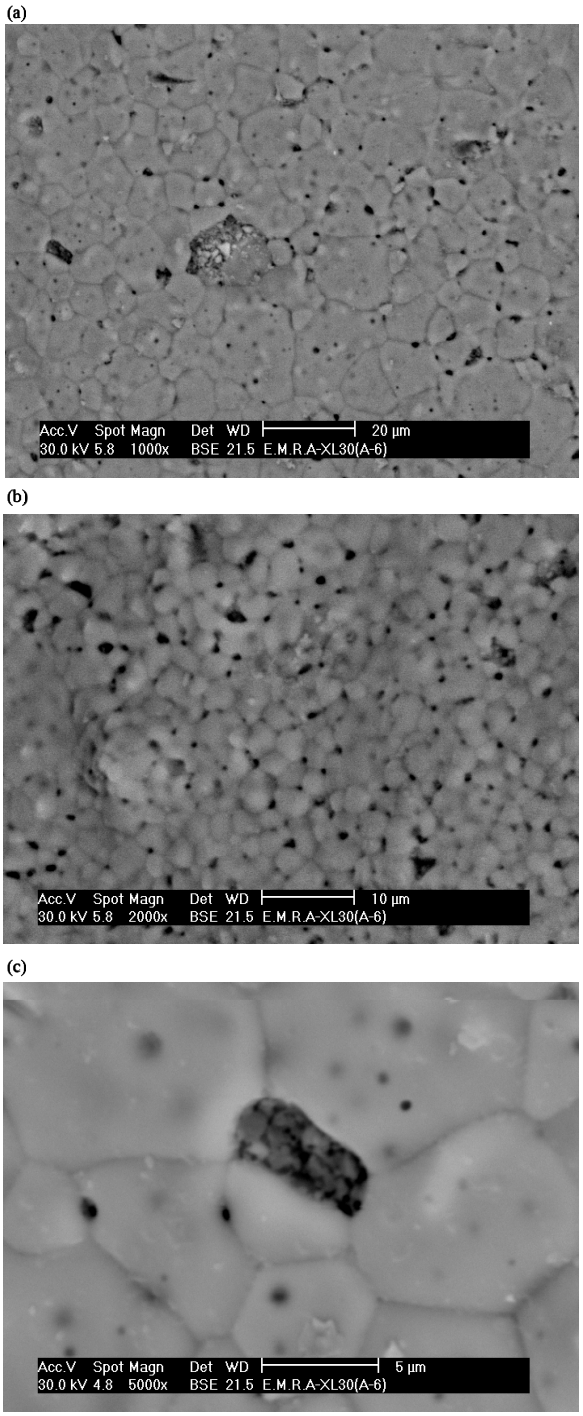

Fig. 8: SEM of mix A6, group 2. (a) Thermally etched, showed two phases ZnO grains and intergranular phase at triple point (general view). X = 1000, (b) Thermally etched, ZnO-ZnO grains and the presence of pores X = 2000 and (c) Thermally etched, ZnO-ZnO grains and the presence of solid solution at triple point. X = 5000

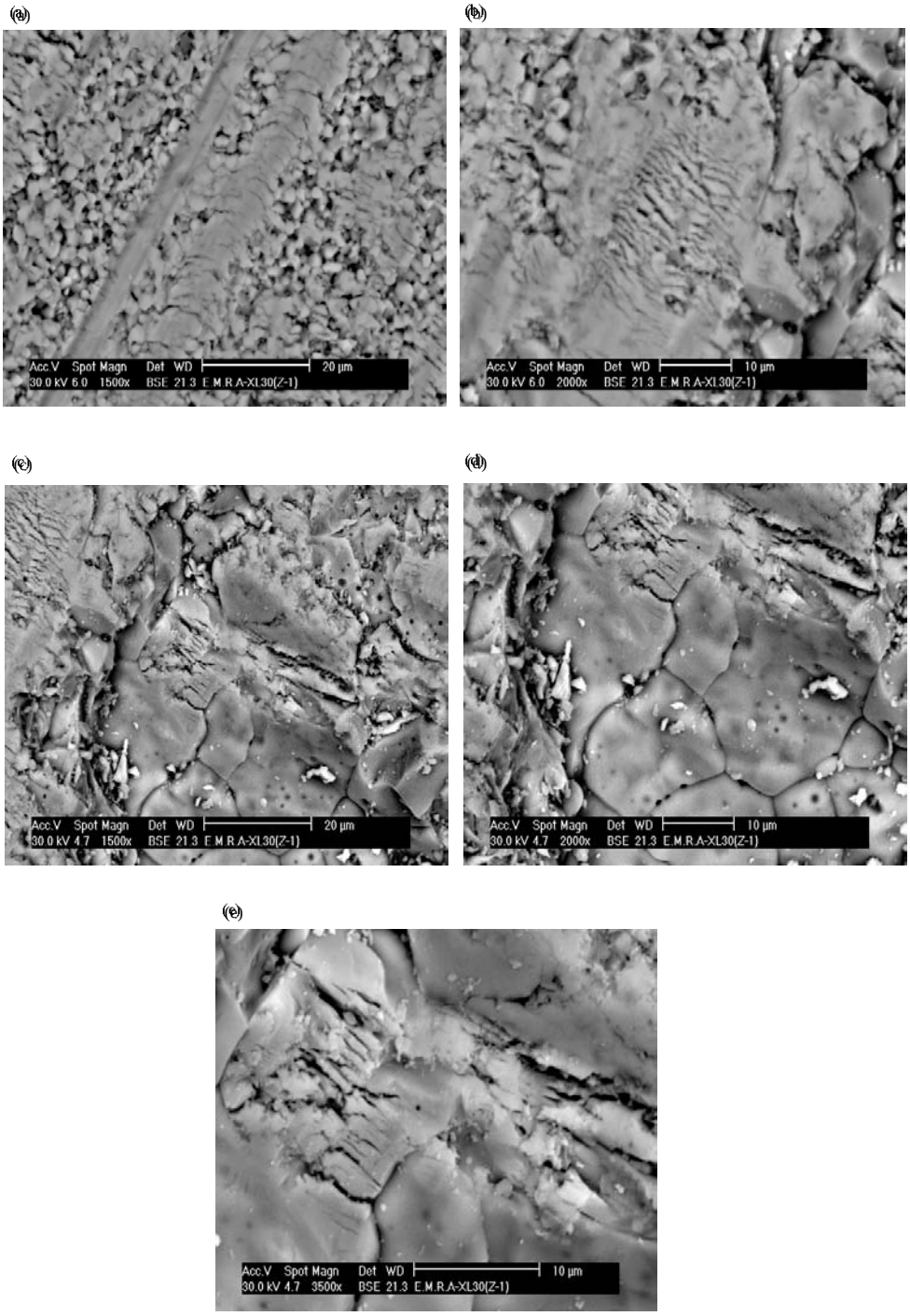

Fig. 9: SEM of mix Z1, group (III). (a) General view of Z1. X = 1500, (b) Thermally etched, growth in preferred orientation in ZnO grains, X = 2000, (c) Thermally etched surface, X= 1500, showing crystal growth of ZnO grains, (d) Amplification of above image X = 2000, ZnO-ZnO grains, liquid phase and the presence of pores and various size. Segregation along grain boundaries X = 3500

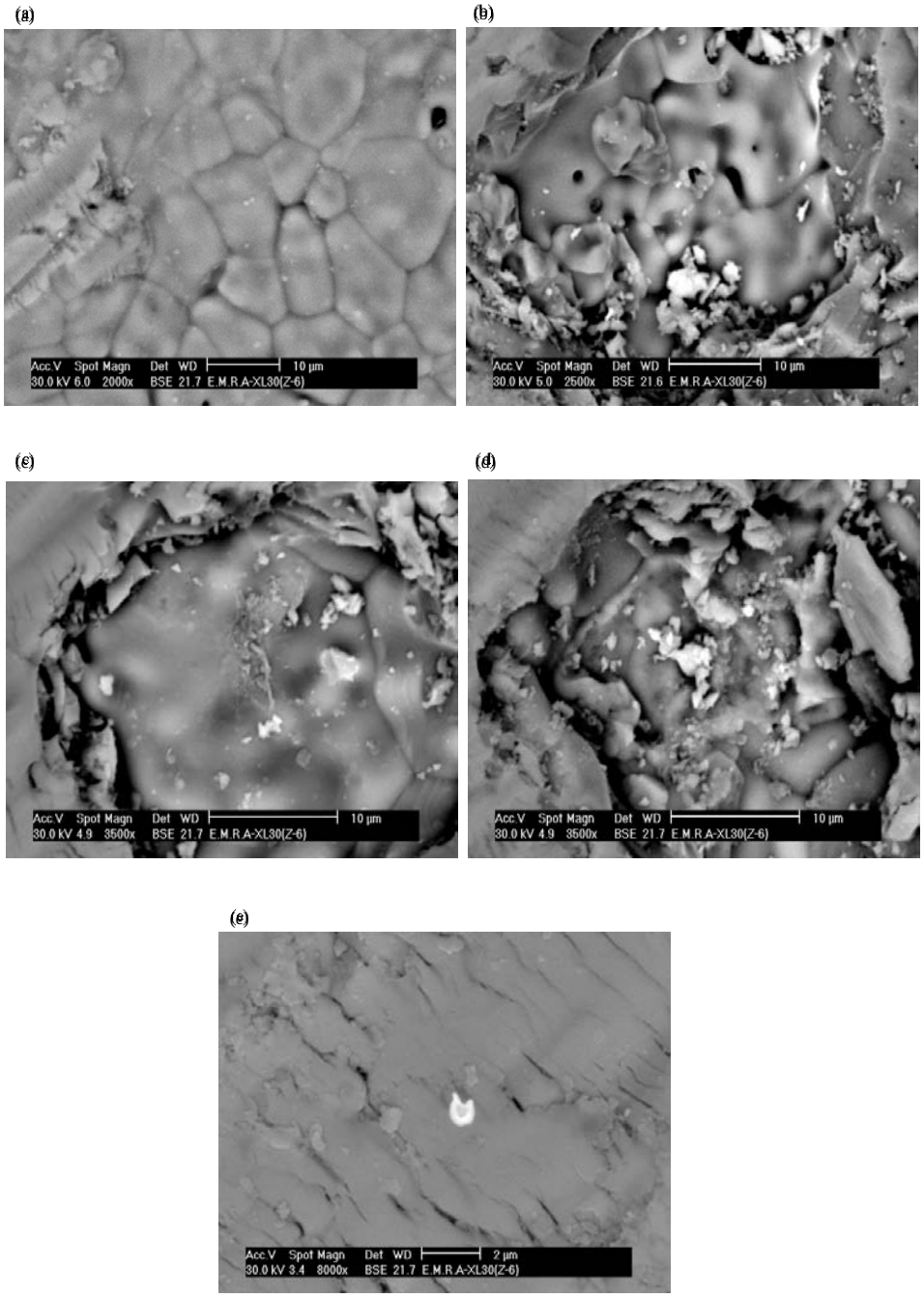

Fig. 10: SEM of mix Z6, group (III). (a) Thermally etched surface, X= 2000, showing crystal growth of ZnO grains and the presence of liquid phase, (b) Thermally etched ZnO grains and intergranular Bi- rich phase. X = 2500, (c) Thermally etched, grain growth of ZnO and intergranular Cu & Bi- rich phase. X = 3500, (d) Thermally etched, showing ZnO grains and exsolution in the triple point and distribution concerted on the pores and (e) Thermally etched, showing contact surfaces between ZnO grains and presence of exsolution of Bi- rich particles

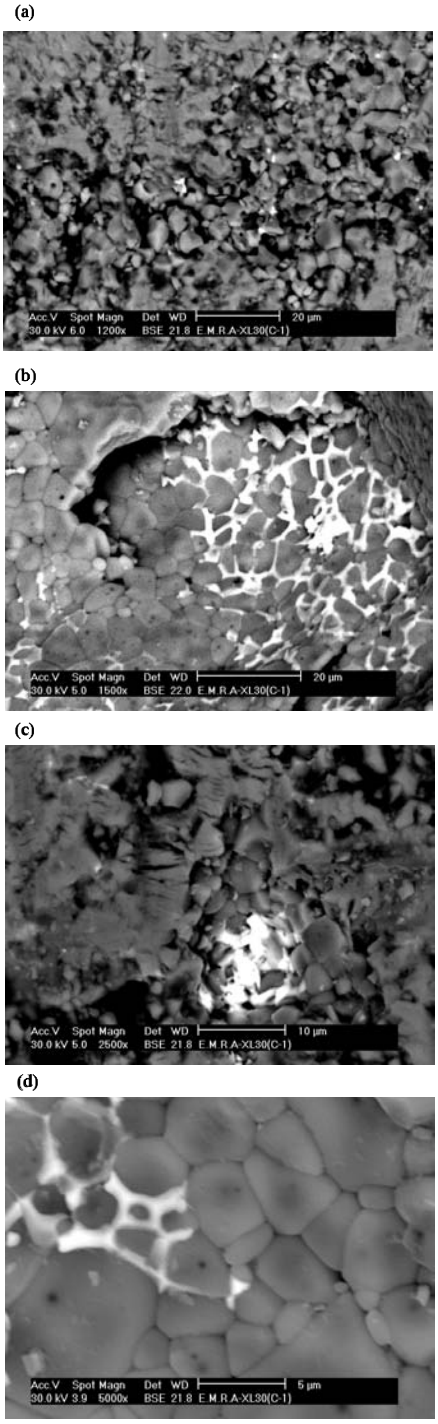

Fig. 11: SEM of mix C_1, group (IV). (a) Thermally etched, general view. X= 1200, (b) Thermally etched, showed two phases ZnO grains and intergranular phase at triple point. X= 1500, (c) Thermally etched, growth in preferred orientation in ZnO grains, X = 2500 and (d) Thermally etched, growth of ZnO grains in preferred orientation. Exsolution of (Ni) rich phase along the grains and intergranular

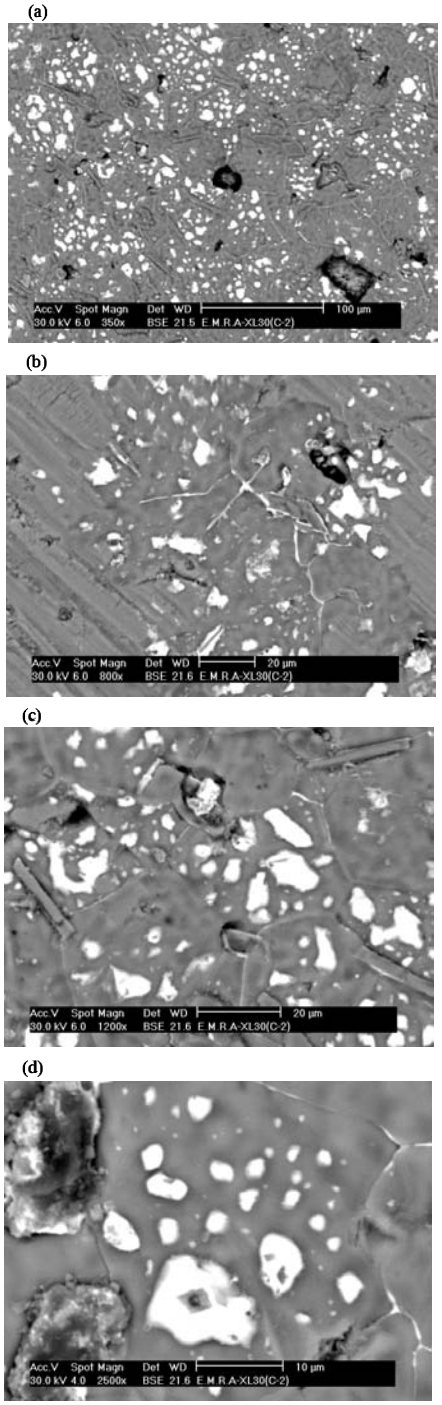

Fig. 12: SEM of mix C_6, group (IV). (a) Thermally etched, general view. X = 350, (b) Thermally etched, Prismatic grains X = 800, (c) Thermally etched, Shows different of prismatic grains, randomly oriented, X = 1200 and (d) Thermally etched, shows two phases ZnO grains and intergranular phase at triple point, Zn is exsoluted accumulating at grain boundaries (white colour), grain growth is evident. X = 2500

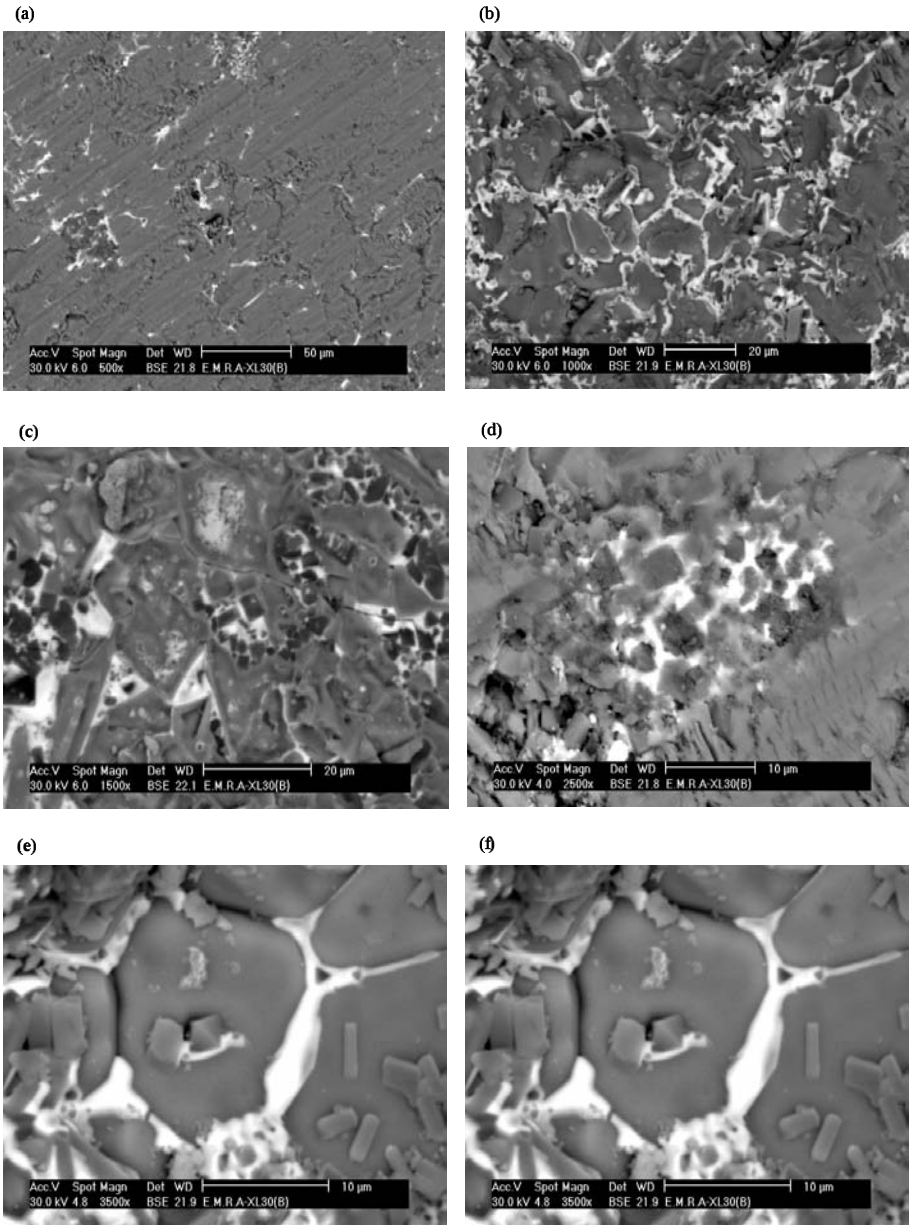

Fig. 13: SEM of mix B, group (V). (a) Thermally etched, general view. X= 500, (b) Thermally etched, ZnO grains and intergranular grains between ZnO grains, X = 1000, (c) Thermally etched, showing ZnO and accumulated phase at triple point, X = 1500, (d) Thermally etched, shows, ZnO grains and Bi- rich phase between grains of ZnO melt liquid phase on the grain boundary. X = 2500, (e) Thermally etched, showing different shapes of prismatic grains of ZnO, Bi in the triple point and the presence of liquid phase on the grain boundary. X= 3500 and (f) Thermally etched, different shapes of ZnO grains, the exsolution of Bi- rich granules along the grain boundary, in various sizes. X = 3500

SEM of mix Z_6 which containing ZnO, 4% mol CuO and 0.5% mol Bi_2O_3 present in Fig. 10, shows crystal growth of ZnO represented by annular epitaxial tiny exsolution of Bi-rich particles, lying intergranular and along the growth rings. Grain growth of ZnO-ZnO grains, liquid phase and exsolution in the triple point and distribution concerted on the pores.

SEM of mix C_1 which containing ZnO, 0.3% mol CuO and 0.5% mol NiO present in Fig. 11, shows crystal growth of ZnO represented by annular epitaxial tiny exsolution of Ni-rich phase, lying intergranular and along the growth rings. Ni and Cu go into solid solution in the ZnO grains and some of the Zn is exsolution accumulating at the grain boundaries or triple point (white in color) grain growth is evident.

SEM of mix C_6 which containing ZnO, 4 mol % CuO and 0.5 mol % NiO present in Fig. 12, shows two phases, ZnO grains and intergranular phase at triple point, also Ni, Cu go into solid solution in the ZnO grains. There are different of prismatic grains, randomly oriented, Zn is exsoluted accumulating at grain boundaries (white color), grain growth is evident.

SEM of mix B which containing ZnO, 6% mol CuO, 0.5% mol Cr_2O_3, 0.5% mol Na_3BiO_3 and 0.5% mol NiO present in Fig. 13, shows different shapes of prismatic grains of ZnO, Bi-rich phase in the triple point and increase the presence of liquid phase (melt liquid phase) on the grain boundary.

CONCLUSIONS

Zno-based varistors were prepared with different CuO content by ball milling sintered at temperature in the range of 900 to 1200°C and characterized by the microstructure, electrical properties and density. With increasing CuO content, the nonlinear coefficient (α) increases and density increase. The presence of a liquid phase facilitated the sintering process and developed atomically interfaces, uniform intergranular phase required for non-linear conduction. The presence of Cr_2O_3 in group (II) absent of grain growth (inhibition of grain growth) and enter in solid solution with ZnO. X-ray diffraction analysis of sintered samples reveals no formation of new phases, but lattice constants of the phases were changed after sintering.

REFERENCES

Antunes, A.C., S.R.M. Antunes, A.J. Zara, S.A. Pianaro, E. Longo and J.A. Varela, 2002. Effect of Fe_2O_3 doping on the electrical properties of a SnO_2 based varistor. J. Mater. Sci., 37: 2407-2411.

Batzill, M. and U. Diebold, 2005. The surface and materials science of tin oxide. Prog. Surf. Sci., 79: 47-154.

Bernik, S., S. Macek and A. Bui, 2004. The characteristics of ZnO-Bi_2O_3-based varistor ceramics doped with Y_2O_3 and varying amounts of Sb_2O_3. J. Eur. Ceram. Soc., 24: 1195-1198.

Bernik, S. and N. Daneu, 2007. Characteristics of ZnO-based varistor ceramics doped with Al_2O_3. J. Eur. Ceram. Soc., 27: 3161-3170.

Bueno, P.R., J.A. Varela, C.M. Barrado, E. Longo and E.R. Leite, 2005. A Comparative study of thermal conductivity in ZnO and SnO_2 based varistor systems. J. Am. Ceram. Soc., 88: 2629-2631.

Cong, L., X. Zheng, P. Hu and S. Dan-Feng, 2007. Bi_2O_3 vaporization in microwave-sintered ZnO varistors. J. Am. Ceram. Soc., 90: 2791-2794.

De la Rubia, M.A., M. Peiteado, J.F. Fernandez and A.C. Caballero, 2004. Compact shape as a relevant parameter for sintering ZnO-Bi_2O_3 based varsitors. J. Eur. Ceram. Soc., 24: 1209-1212.

Fayat, J. and M.S. Castro, 2003. Defect profile and microstructural development in SnO_2-based varistors. J. Eur. Ceram. Soc., 23: 1585-1591.

Glot, A.B., 2006a. A simple approach to oxide varistor materials. J. Mater. Sci., 41: 5709-5711.

Glot, A.B., 2006b. A model of non-ohmic conduction in ZnO varistors. J. Mater. Sci.: Mater. Electron., 17: 755-765.

Glot, A.B. and I.A. Skuratovsky, 2006. Non-ohmic conduction in tin dioxide based varistor ceramics. Mater. Chem. Phys., 99: 487-493.

Leach, C., 2005. Grain boundary structures in zinc oxide varistors. Acta Materialia, 53: 237-245.

Li, S.T., J.Y. Li, F.Y. Liu, M.A. Alim and G. Chen, 2002. The dimensional effect of breakdown field in ZnO varistors. J. Phys. D: Applied Phys., 35: 1884-1888.

Lin, C.C., W.S. Lee, C.C. Sun and W.H. Whu, 2007. The influences of bismuth antimony additives and cobalt manganese dopants on the electrical properties of ZnO based varistors. Compos. Part B, 38: 338-344.

Metz, R., J. Morel, M. Houabes, J. Pansiot and M. Hassanzadeh, 2007. High voltage characterization of tin oxide varistors. J. Mater. Sci., 42: 10284-10287.

Nahm, C.W., 2004. Effect of cooling rate on degradation characteristics of $ZnO{\bullet}Pr_6O_{11}{\bullet}CoO{\bullet}Cr_2O_3{\bullet}Y_2O_3$-based varistors. Solid State Commun., 132: 213-218.

Nahm, C.W., 2007. The effect of sintering temperature on electrical properties and accelerated aging behavior of PCCL-doped ZnO varistors. Mater. Sci. Eng. B, 136: 134-139.

Oliveira, M.M., P.C. Soares J.r., P.R. Bueno, E.R. Leite, E. Longo and J.A. Varela, 2003. Grain-boundary segregation and precipitates in La_2O_3 and Pr_2O_3 doped SnO_2.CoO based varistors. J. Eur. Ceram. Soc., 23: 1875-1880.

Ott, J., A. Lorenz, M. Harrer, E.A. Preissner and C. Hesse, 2001. The influence of Bi_2O_3 and Sb_2O_3 on the electrical properties of ZnO-based varistors. J. Electroceram., 6: 135-146.

Parra, R., M.S. Castro and J.A. Varela, 2005. Analysis of secondary phases segregated and precipitated in SnO_2-based varistors. J. Eur. Ceram. Soc., 25: 401-406.

Peiteado, M., M.A. de la Rubia, M.J. Velasco, F.J. Valle and A.C. Caballero, 2005. Bi_2O_3 vaporization from ZnO-based varistors. J. Eur. Ceramic. Soc., 25: 1675-1680.

Ramirez, M.A., P.R. Bueno, W.C. Ribeiro, D.A. Bonett and J.M. Villa *et al.*, 2005. The failure analyses on ZnO varistors used in high tension devices. J. Mater. Sci., 40: 5591-5596.

Santos, M.R.C., P.R. Bueno, E. Longo and J.A. Varela, 2001. Effect of oxidizing and reducing atmosphere on the electrical properties of dense SnO_2 based varistors. J. Eur. Ceram. Soc., 21: 161-167.

Simoes, L.G.P., P.R. Bueno, M.O. Orlandi, E.R. Leite and E. Longo, 2003. The influence of excess precipitate on the non-ohmic properties of SnO_2 based varistors. J. Electroceram., 10: 63-68.

Skuratovsky, I., A. Glot, E. Di Bartolomeo, E. Traversa and R. Polini, 2004. The effect of humidity on the voltage-current characteristic of SnO_2 based ceramic varistor. J. Eur. Ceram. Soc., 24: 2597-2604.

Skuratovsky, I., A. Glot and E. Traversa, 2006. Modelling of the humidity effect on the barrier height in SnO_2 varistors. Mater. Sci. Eng. B, 128: 130-137.

So, S.J. and C.B. Park, 2002. Improvement in the electrical stability of semiconducting ZnO ceramic varistors with SiO_2 additive. J. Korean Phys. Soc., 40: 925-929.

Souza, F.L., J.W. Gomes, P.R. Bueno, M.R. Cassia-Santos and A.L. Araujo *et al.*, 2003. Effect of the addition of ZnO seeds on the electrical proprieties of ZnO-based varistors. Mater. Chem. Phys., 80: 512-516.

Takemura, T., M. Kobayashi, Y. Takada and K. Sato, 1986. Effects of bismuth sesquioxide on the characteristics of ZnO varistors. J. Am. Ceram. Soc., 69: 430-436.

Tong, Y.L., W.Z. Hong, D. Liang, G. Na and W. Yu, 2009. Novel varistor material based on terbium oxide. J. Phys. D: Applied Phys., 42: 1-4.

Wang, Y.J., J.F. Wang, C.P. Li, H.C. Chen and W.B. Su *et al.*, 2000. Improved varistor nonlinearity via sintering and acceptor impurity doping. Eur. Phys. J. Applied Phys., 11: 155-158.

Wang, W.X., J.F. Wang, H.C. Chen, W.B. Su and G.Z. Zang, 2003. Electrical nonlinearity of (Cu, Ni, Nb)-doped SnO_2 varistors system. Mater. Sci. Eng. B, 99: 457-460.

Wang, C.M., J.F. Wang, H.C. Chen, W.B. Su, G.Z. Zang, P. Qi and M.L. Zhao, 2005. Effects of CuO on the grain size and electrical properties of SnO_2-based varistors. Mater. Sci. Eng. B, 116: 54-58.

Wu, Z.H., J.H. Fang, D. Xu, Q.D. Zhong and L.Y. Shi, 2010. Effect of SiO_2 addition on the microstructure and electrical properties of ZnO-based varistors. Int. J. Minerals Metallurgy Mater., 17: 86-91.

Yongjun, W., W. Jinfeng, C. Hongcun, Z. Weilie, Z. Peilin, D. Huomin and Z. Lianyi, 2000. Electrical properties of SnO_2-ZnO-Nb_2O_5 varistor system. J. Phys. D: Applied Phys., 33: 96-99.